



EXPERIMENTAL STUDY ON THE REPAIR EFFECT OF RC PIERS DAMAGED BY EARTHQUAKES

Kazunori Watanabe¹, Kenji Ikeda², Norimitsu Kishi³, Tadashi Hasegawa⁴

SUMMARY

Cyclic loading tests using specimens approximately one-fourth the size of an actual structure were conducted for quantitative measurement of the repair effect depending on the degree of damage in the case of repair of an RC pier damaged by an earthquake. In the loading tests, specimens to which a certain amount of damage was inflicted through preliminary loading were repaired by the injection of epoxy resin or section restoration using non-shrink mortar, and load was then applied once again. The experiment revealed that tenacity and energy absorption could be improved in the repaired specimens and that their seismic performance could be equivalent to or higher than the specimens that had not been repaired, although the rigidity decreased up until the first yield displacement.

INTRODUCTION

Many RC piers were severely damaged by the Hyogo-ken Nambu Earthquake (Great Hanshin-Awaji Earthquake) that occurred in 1995. Many of the damaged piers had been designed many years before and had little hoop reinforcement. Under these circumstances, the importance of plastic deformation performance after member yielding was pointed out, and aseismic design based on the new criteria with emphasis on plastic deformation performance was introduced in Japan, in addition to the conventional aseismic design employing the seismic intensity method¹⁾. Introduction of this design method has since then dramatically improved the earthquake performance of RC piers.

Allowance of damage in the plastic range, however, means that it is necessary to conduct repair for restoration of functions in order to put the structure back into service after the earthquake.

Also, the repair effect of damaged RC piers has not been measured quantitatively although experimental studies^{2) 3)} are currently being conducted concerning the repair of such piers. The authors determined that quantitative measurement of the seismic performance and repair effect of RC piers after being damaged could lead to the realization of rational and economical repair methods, and therefore conducted evaluation and examination of repair and recovery by producing wall-type RC pier specimens approximately one-fourth the size of an actual structure, inflicting a certain amount of damage to these specimens by preliminary loading and conducting cyclic loading tests.

¹ Researcher, Structure Section, CERI, Sapporo, Japan. Email : watanabe@ceri.go.jp

² Director, Structure Section, CERI, Sapporo, Japan. Email : ikedak@ceri.go.jp

³ Professor, Muroran Institute of Technology, Muroran, Japan

⁴ Project Manager, Chodai Sapporo Branch, Sapporo, Japan

OUTLINE OF THE EXPERIMENT

Experimental method

The wall-type RC pier, which is commonly seen in road bridges, was chosen to be the subject of this study. To reproduce conditions as close as possible to those of an actual structure, cyclic loading tests were conducted while the vertical axial force of 150 kN, which was equivalent to the dead weight of the superstructure, was maintained using a vertical loading jack. Photo 1 shows a view of the experimental equipment. In cyclic loading, the yield strain of the axial reinforcement was first set at 1890μ , which was obtained through material testing. Load was then applied by strain control until the strain of the tension-side reinforcement at the base of the pier reached yield strain.



Photo 1 View of the experimental equipment

The loading point displacement at this point was defined as yield displacement δ_y and the horizontal load was defined as yield load P_y . In the subsequent loading, displacement was controlled by gradually increasing the single amplitude by an integral multiple of the yield displacement ($2\delta_y$, $3\delta_y$...) and the loading was repeated three times for each displacement amplitude.

The ultimate displacement was defined as the loading point displacement of the stage where either positive or negative load became smaller than the yield load P_y at the first loading of each displacement amplitude.

In the case of the repaired specimens, a certain amount of damage was inflicted through cyclic loading as preliminary loading before the repair was made, the cracked parts were repaired by epoxy resin injection or section restoration using non-shrink mortar while maintaining the zero displacement and cyclic loading tests were conducted once again.

Because the strain gauge of the main reinforcement became unusable during the preliminary loading stage in the case of the repaired specimens, yield displacement δ_y of the standard specimen without repair was used as the standard displacement for cyclic loading.

Outline of specimens and repair

The specimens were constructed to simulate the wall-type RC pier, which is commonly seen in road bridges, and their size was approximately one-fourth that of an actual pier. Figure 2 shows a schematic diagram of the reinforcement arrangement of the specimens.

The specimens had rectangular sections (aspect ratio of side length 1:3) with a height of 2.0 m and section size of 0.38×1.14 m. The tensile reinforcement ratio was $P_t = 0.45\%$ and the volume ratio of the hoop reinforcement was $\rho_s = 0.2\%$.

Specimens to be repaired were supposed to be in the following three stages of damage before repair:

1) The stage with only horizontal cracking, 2) the stage before concrete cover began to swell and 3) the level at which the concrete cover had exfoliated and the reinforcement was buckled.

Based on the damage conditions in load testing of the standard specimen, a preliminary load of up to $3\delta_y$, $5\delta_y$ and $7\delta_y$ was applied, respectively. After that, repair was conducted under the condition in which the displacement was forcibly returned to zero, and the main load was applied.

Table 1 lists the specimens used. In the table, the first part of the name of each specimen shows the height of the specimen, the second part indicates the repair condition (N: no repair, R: resin injection, M: sectional restoration) and the third part represents the maximum displacement amplitude at the preliminary loading stage. Five specimens were used for the experiment: 2.0-R-3 and 2.0-R-5 for which

epoxy resin was injected into cracks after applying a preliminary load of $3\delta_y$ and $5\delta_y$, respectively; 2.0-M-5 and 2.0-M-7 for which the concrete cover was removed after applying a preliminary load of $5\delta_y$ and $7\delta_y$, respectively, and section restoration was conducted using non-shrink mortar; and 2.0-N, which was employed as the standard specimen.

The repair area was only the part where cracking could be clearly observed. This area was in the range of 300 mm from the base for specimens with a preliminary load of $3\delta_y$ and $5\delta_y$, and 500 mm from the base for specimens with a preliminary load of $7\delta_y$. The size of the section was not increased for any of the specimens.

Also, Table 2 shows the physical properties of the materials used for repair. The mean compressive strength of concrete at the material age at the time of experiment was $f_c = 31.5$ MPa, the mean elastic modulus was 3.18 GPa, reinforcement was SD345 type and the mean yield point strength according to the tension test was 389 Mpa.

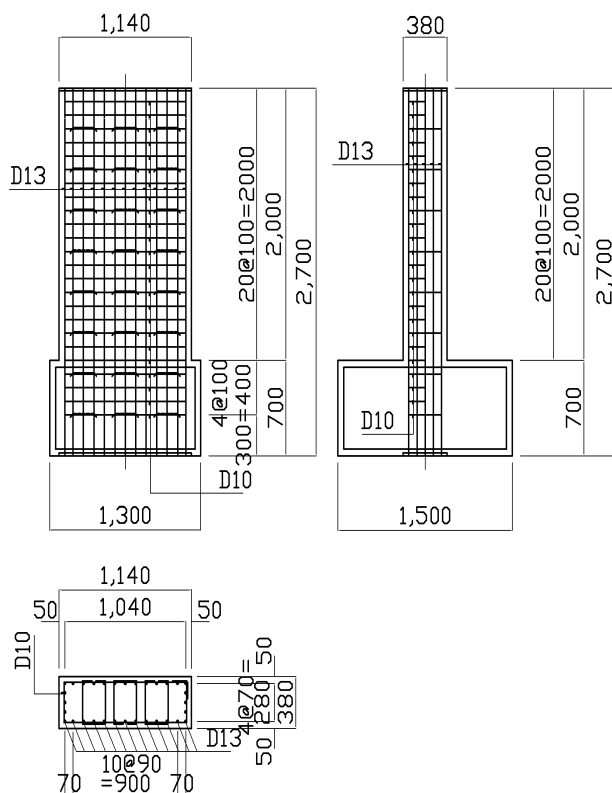


Fig.2 Reinforcement arrangement of the specimens

Table 1 Specimen list

Specimen	preliminary loading	Repair method
2.0-N	-	-
2.0-R-3	$3\delta_y$	Epoxy resin injection
2.0-R-5	$5\delta_y$	Epoxy resin injection
2.0-M-5	$5\delta_y$	Non-shrink mortar sectional restoration
2.0-M-7	$7\delta_y$	Non-shrink mortar sectional restoration

Table 2 List of physical properties for repair materials

Material	Compressive strength (N/mm ²)	Tensile strength (N/mm ²)
Epoxy resin	60.0 or higher	30.0 or higher
Non-shrink mortar	32.6 (Material age:3 days)	

EXPERIMENTAL RESULTS AND CONSIDERATION

Damage conditions of specimens

2.0-N specimen

Damage to the 2.0-N specimen, which was the standard specimen, occurred in the form of horizontal cracking over the range of 1,200 mm from the base, at intervals of approximately 100 mm, in the height direction and at the time of $1\delta_y$ to $3\delta_y$ loading. During and after the $3\delta_y$ loading stage, damage was concentrated within the range of 300 mm from the base, and almost no progress of damage was observed in the section above that. During the $5\delta_y$ loading stage, the exfoliation of the concrete cover due to the loss of adhesion of the axial reinforcement was found using the hammer tap tone, although swelling of the concrete cover was not observed near the base.

After that, the concrete cover began to swell during the $6\delta_y$ loading stage and exfoliated over a wide area at $7\delta_y$. The load decreased at $8\delta_y$ as the main reinforcement was broken and the ultimate stage was reached. The exfoliation of concrete cover occurred within the range of 300 mm from the base. Photo 2 shows the damage condition of the 2.0-N specimen at the ultimate stage.

2.0-R-3 specimen

Damage observed at the end of preliminary loading ($3\delta_y$) was horizontal cracking at intervals of 100 mm in the height direction.

At the time of loading after repair, exfoliation or other damage of concrete cover was not confirmed until the $8\delta_y$ loading stage when the 2.0-N specimen reached the ultimate stage. After that, concrete cover exfoliated over a wide area during the $9-10\delta_y$ loading stage, and the ultimate stage was reached at $11\delta_y$ when the load dramatically decreased due to the breakage of multiple main reinforcement bars during loading.

The exfoliation of concrete cover occurred within the range of approximately 300 mm from the base. Photo 3 shows the damage condition of the 2.0-R-3 specimen at the ultimate stage.

2.0-R-5 specimen

Damage observed at the end of preliminary loading ($5\delta_y$) was the exfoliation of concrete cover within the range of approximately 300 mm from the base.

At the time of loading after repair, exfoliation of or other damage to concrete cover was not confirmed until the $8\delta_y$ loading stage in the same manner as the case of the 2.0-R-3 specimen.

Although the swelling of concrete cover was observed during the $9\delta_y$ loading stage, injected epoxy resin prevented exfoliation of concrete cover, and resulted in a peculiar form of damage in which the exfoliation of concrete cover did not occur even when swelling became significant at $10\delta_y$. Concrete cover exfoliated during the $11\delta_y$ loading stage and the ultimate stage was reached at 12 and $13\delta_y$ when multiple main reinforcement bars were broken.

The extent of the exfoliation of concrete cover was greater compared with the 2.0-N and 2.0-R-3 specimens, and within the range of approximately 500 mm from the base. Photo 4 shows the damage condition of the 2.0-R-5 specimen at the ultimate stage.

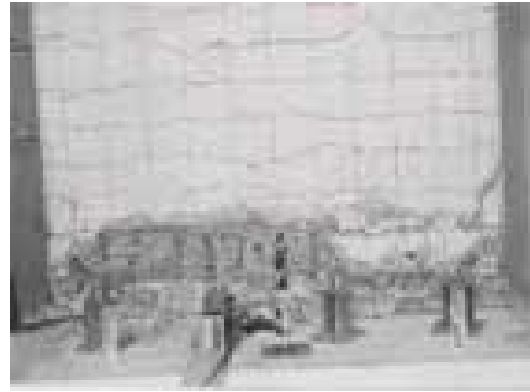


Photo2 Damage condition of the 2.0-N specimen

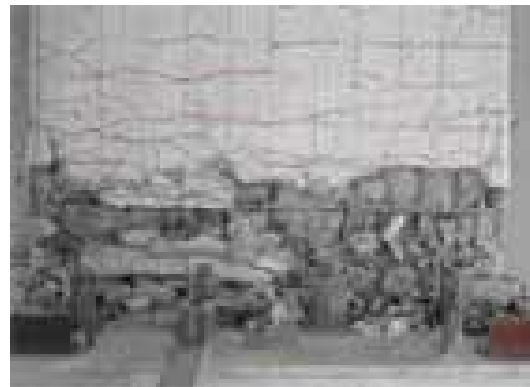


Photo3 Damage condition of the 2.0-R-3 specimen



Photo4 Damage condition of the 2.0-R-5 specimen

2.0-M-5 specimen

Damage observed at the end of preliminary loading ($5\delta_y$) was the exfoliation of concrete cover within the range of approximately 300 mm from the base, in the same manner as the 2.0-R-5 specimen.

At the time of loading after repair, the expansion of the width of cracks was observed at the boundary between the non-shrink mortar part and the existing part during the $6\delta_y$ loading stage. Swelling of non-shrink mortar occurred during the $8\delta_y$ loading stage and the mortar exfoliated over a wide area during the $9\delta_y$ loading stage. The load gradually decreased through subsequent loading, and the ultimate stage was reached at $11\delta_y$.

The exfoliation of concrete cover occurred only within the range of 300 mm from the base where the section was restored, and the boundary between exfoliated and existing parts was clear. Photo 5 shows the damage condition of the 2.0-M-5 specimen at the ultimate stage.

2.0-M-7 specimen

Damage observed at the end of preliminary loading ($7\delta_y$) was the exfoliation of concrete cover within the range of 300 mm from the base. The main reinforcement was already buckled and the exfoliation of concrete cover was observed within the range of 500 mm from the base.

At the time of loading after repair, partial exfoliation occurred in the non-shrink mortar of the repaired part after the $5\delta_y$ loading stage. After that, the range of exfoliation gradually expanded with the increase in displacement amplitude.

Non-shrink mortar exfoliated over a wide area, the load decreased during the $9\delta_y$ loading stage and the ultimate stage was reached at $11\delta_y$.

The exfoliation of concrete cover only occurred within the range of 500 mm from the base where the section was restored, and the boundary between the exfoliated and existing parts was clear. Photo 6 shows the damage condition of the 2.0-M-7 specimen at the ultimate stage.



Photo5 Damage condition of the 2.0-M-5 specimen



Photo6 Damage condition of the 2.0-M-7 specimen

Load-displacement relationship

Table 3 shows the list of experimental results and Fig. 3 shows the envelope of the load-displacement relationship (first stage of repeat loading, mean push-pull values). In the table, δ_y and P_y represent the horizontal displacement at the loading point and the load at the time of yield of the main reinforcement, respectively; P_a is the maximum load (mean push-pull values) and δ_u is the horizontal displacement at the ultimate stage.

The table and figure show that, for all of the specimens after repair, the load P_y during the $1\delta_y$ loading stage was as small as 76 to 80% of that of the 2.0-N specimen, indicating that the initial rigidity was decreasing. This is probably because repair was only conducted for visible cracks and where resin injection was possible, and hair cracks and other fine cracks were not repaired. In addition, in the case of mortar repair, only the section restoration part was repaired.

During the $2\delta_y$ loading stage, the load of repaired specimens was larger than that of 2.0-N and the maximum load P_a also increased by 5 to 7%.

It can also be seen that the load on the 2.0-M-7 specimen gradually decreased after $5\delta_y$, when the exfoliation of non-shrink mortar occurred. On the other hand, the load did not decrease for the 2.0-R-3, 2.0-R-5 and 2.0-M-5 specimens even during the $8\delta_y$ loading stage when the 2.0-N specimen reached the ultimate stage.

The ultimate plasticity, which is evaluated by dividing ultimate displacement δ_u by yield displacement δ_y , was 11 for 2.0-R-3, 2.0-M-5 and 2.0-M-7 and 13 for 2.0-R-5, while it was 8 for the 2.0-N specimen, thereby indicating that tenacity increased dramatically compared with that before repair.

Figure 4 presents the load-displacement relationship from the beginning of loading to $1\delta_y$. The figure shows that, in the 2.0-N specimen, there was a clear difference in rigidity before (displacement: 0 – 3mm) and after the occurrence of cracking (displacement: 3 – 12mm). It can also be seen that the rigidity of repaired specimens from the beginning of loading was almost equivalent to that after the occurrence of cracking in 2.0-N. In the same way as mentioned above, it was probably because hair cracks and other fine cracks, for which resin injection was impossible, remained due to unloading after preliminary loading in 2.0-R-3 and 2.0-R-5, and because cracks outside the section restoration part were not repaired in the 2.0-M-5 and 2.0-M-7 specimens.

The starting points of loading differ in the figure because of the effect of the initial input caused by repair conducted while the displacement was maintained at zero.

Table 3 List of experimental results

Specimen	Displacement (mm)		Load (kN)		Ultimate Plasticity
	δ_y	δ_u	P_y	P_a	
2.0-N	12.2	97.6	94	126	8
2.0-R-3	12.2	134.2	76	131	11
2.0-R-5	12.2	158.6	74	132	13
2.0-M-5	12.2	134.2	76	135	11
2.0-M-7	12.2	134.2	72	133	11

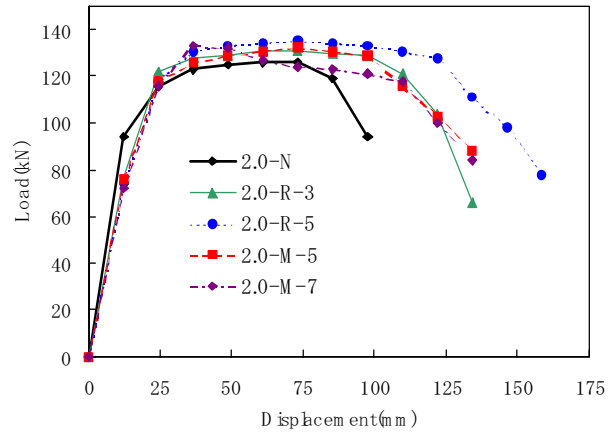


Fig.3 Load-displacement relation envelope

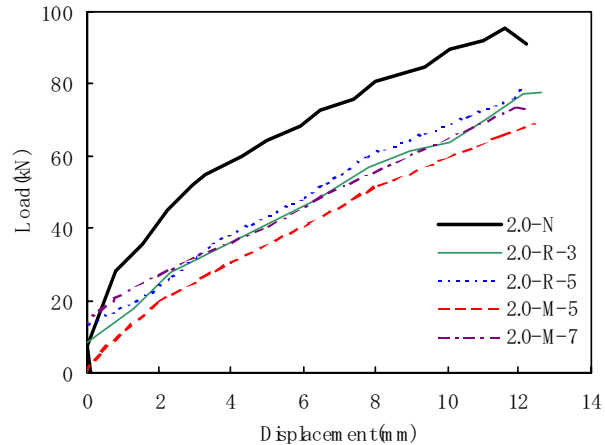


Fig.4 Load-displacement relation envelope (up to $1\delta_y$)

Hysteresis absorbed energy

Figure 5 shows the relationship between the accumulated amount of hysteresis absorbed energy and displacement amplitude (δ/δ_y) up to the ultimate displacement of each specimen.

While the accumulated amount of hysteresis absorbed energy at the ultimate stage was 200.2 kNmm ($8\delta_y$) for the 2.0-N specimen, it was 366.6 kNmm ($11\delta_y$) for 2.0-R-3, 531.8 kNmm ($13\delta_y$) for 2.0-R-5, 371.7 kNmm ($11\delta_y$) for 2.0-M-5 and 274.9 kNmm ($11\delta_y$) for 2.0-M-7. These values were 1.4 to 2.6 times as large as that of the standard specimen.

Focusing on the $8\delta_y$ loading stage when the 2.0-N specimen reached the ultimate stage, however, the hysteresis absorbed energy was low after $5\delta_y$ when the exfoliation of concrete cover occurred in 2.0-M-7 and the accumulated value was approximately 80% of that of 2.0-N, while the values for 2.0-R-3, 2.0-R-5 and 2.0-M-5 were 1.1 to 1.2 times as high as that of 2.0-N.

It was thus revealed that, at $8\delta_y$ loading in which the standard specimen 2.0-N reached the ultimate stage, the amount of hysteresis absorbed energy was higher if the degree of damage before repair was low and that hysteresis absorbed energy equivalent to or higher than that before repair was observed in specimens for which repair was conducted at a stage before swelling of the concrete cover began.

Equivalent viscous damping constant

Figure 6 shows the equivalent viscous damping constant that can be calculated from the hysteresis curve of each displacement amplitude.

The equivalent viscous damping constant h_{eq} of 2.0-N, which was the standard specimen, increased gradually from 11% during the $1\delta_y$ loading stage to the maximum of 26%.

While the value of 2.0-R-3 was smaller than that of 2.0-N until the $6\delta_y$ loading stage, the value became larger than that of 2.0-N during and after the $7\delta_y$ loading stage, and the maximum value was 29%.

While the value of 2.0-R-5 was smaller than that of 2.0-N until the $7\delta_y$ loading stage, the value became larger than that of 2.0-N during and after the $8\delta_y$ loading stage. After exhibiting the maximum value of 31% during the $10\delta_y$ loading stage, the value began to decrease and reached as low as 22% at the ultimate stage of $13\delta_y$.

For 2.0-M-5, the value was smaller than that of 2.0-N until the $6\delta_y$ loading stage, and became larger than that of 2.0-N during and after the $7\delta_y$ loading stage. The maximum value was 28%.

Comparing the 2.0-R-5 and 2.0-M-5 specimens, it can be seen that the value of mortar repair was larger up to $9\delta_y$, and that of resin injection became larger after that.

The values for 2.0-M-7 tended to be smaller compared with other specimens, and it can be seen that the increase became smaller after the $5\delta_y$ loading stage, and h_{eq} was 10 to 21%. This is probably due to the occurrence of buckling in the main reinforcement during the preliminary loading stage and the exfoliation of non-shrink mortar after the $5\delta_y$ loading stage.

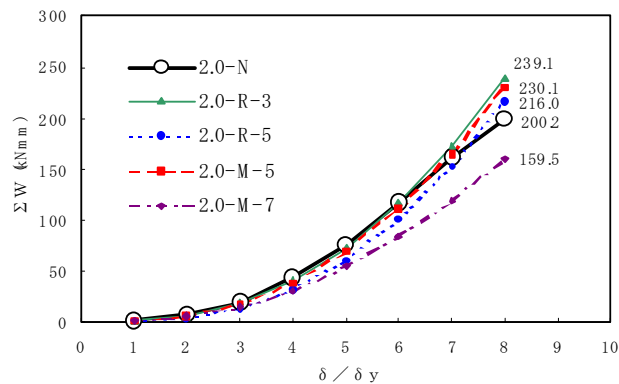


Fig.5 Hysteresis absorbed energy (in the terminal stage)

CONCLUSION

A loading experiment was conducted using RC pier specimens, which were repaired after preliminary loading, to establish rational and economical repair technology for damaged RC piers. The results obtained through this study can be summarized as follows:

- 1) Repair by injection of epoxy resin and sectional restoration using non-shrink mortar can recover the deformation performance to a higher level than before making the repair. The value of horizontal load also exceeded that before the repair during and after the 2 δ_y loading stage.
- 2) The value of load at the time of yield displacement decreased to 76 – 80% of that before the repair because fine cracks remained.
- 3) In the case in which exfoliation of concrete cover occurred at the preliminary loading stage, energy absorption and damping performance did not recover to the level before the repair, although ultimate plasticity was improved.

REFERENCES

1. Japanese Specifications for Highway Bridges and manuals, V-aseismic design, 1996 edition, Dec. 1996.
2. Umihara et al.: Test results concerning the repair effect of high-toughness RC columns damaged by cyclic loading in the large deformation zone, 2nd Symposium on Earthquake-Proof Strengthening and Repair Technology and Earthquake-Proof Diagnosis Technology, pp.71 – 78, July 1998.
3. Suzuki and Hirasawa: A basic experiment on the repair effect of RC square-section columns, summary of the 51st Annual Academic Lecture of the Japan Society of Civil Engineers, pp.1128 – 1129, Sept. 1996.